RESEARCH ARTICLE

[M]acro-
olecular
Materials and Engineering
Open Access
www.mame-journal.de

Tailoring the Surface Chemistry of PEDOT:PSS to Promote Supported Lipid Bilayer Formation

Konstantinos Kallitsis, Anna-Maria Pappa, Zixuan Lu, Alberto Alvarez-Fernandez, Ioanna Charalambous, Sina Schack, Walther C. Traberg, Quentin Thiburce, Karan Bali, Graham Christie, Stefan Guldin, Susan Daniel, Alberto Salleo, and Róisín M. Owens*

This communication reports on a versatile and substrate-agnostic method to tune the surface chemistry of conducting polymers with the aim of bridging the chemical mismatch between bioelectronic devices and biological systems. As a proof of concept, the surface of poly(3,4-ethylenedioxythiophene) polystyrene sulfonate (PEDOT:PSS) is grafted with a short-chain oligoethylene glycol monolayer to favor the formation of cell-derived supported lipid bilayers (SLBs). This method is tuned to optimize the affinity between the supported lipid bilayer and the conducting polymer, leading to significant improvements in bilayer quality and therefore electronic readouts. To validate the impact of surface functionalization on the system's ability to transduce biological phenomena into quantifiable electronic signals, the activity of a virus commonly used as a surrogate for SARS-CoV-2 (mouse hepatitis virus) is monitored with and without surface treatment. The functionalized devices exhibit significant improvements in electronic output, stemming from the improved SLB quality, therefore strengthening the case for the use of such an approach in membrane-on-a-chip systems.

1. Introduction

Supported lipid bilayers (SLBs) represent one of the simplest and most reliable models for studying the interaction of cells with their environment. Since their first report in the mid-1980s,[1] they have been gradually gaining in complexity, modeling cell membranes with ever higher fidelity.[2] While initial efforts focused on the reconstitution of plasma membranes using synthetic components, the leap toward biomimetic SLBs came with the rupture of cell material containing all the complexity found in the native plasma membrane.[2b] The resulting SLBs, made via rupture of extracellular vesicles (blebs) on flat substrates, contain the proteins found on the surface of the cells, with the correct orientation and transmembrane mobility, all essential for their proper functionality. Such native plasma membranes can be used to study specific proteins in a native membrane environment (i.e., without any prior genetic modification of the cell), or enhanced by overexpression, hence serving as a viable alternative to whole-cell studies in assessing biological events that occur at the first point of contact with proteins, the plasma membrane.[3]

The recent coupling of this technology with conducting polymers (CP) yields a new generation of biomimetic

K. Kallitsis, A.-M. Pappa, Z. Lu, I. Charalambous, S. Schack,
W. C. Traberg, K. Bali, G. Christie, R. M. Owens
Department of Chemical Engineering and Biotechnology
University of Cambridge
CB3 0AS Cambridge, UK
E-mail: zl422@cam.ac.uk; rmo37@cam.ac.uk
A.-M. Pappa
Department of Biomedical Engineering
Khalifa University of Science and Technology & Healthcare Engineering
Innovation Center
PO BOX 127788 Abu Dhabi, United Arab Emirates

A.-M. Pappa
Healthcare Engineering Innovation Center (HEIC)
Khalifa University of Science and Technology
PO Box 127788 Abu Dhabi, United Arab Emirates
A. Alvarez-Fernandez, S. Guldin
Department of Chemical Engineering
University College London
WC1E 7JE London, UK
Q. Thiburce, A. Salleo
Department of Materials Science and Engineering
Stanford University
Stanford, CA 94305, USA
S. Daniel
Robert F. Smith School of Chemical and Biomolecular Engineering
Cornell University
Olin Hall, Ithaca, NY 14853, USA

**ADVANCED
SCIENCE NEWS**

www.advancedsciencenews.com

[M] acro-
olecular
Materials and Engineering
Open Access

www.mame-journal.de

bioelectronic devices[4] with the capability of real-time electrical recordings and signal quantification, both challenging using the state-of-the-art methods for SLB characterization.[2b] Additionally, the hydrogel-like properties of conducting polymers such as poly(3,4-ethylenedioxythiophene) polystyrene sulfonate (PEDOT:PSS) provide a biomimetic environment for the native SLBs, facilitating membrane and transmembrane protein mobility, by acting as a cushion.[5] However, there are still challenges when it comes to using the vesicle fusion method[6] on conducting polymer-based surfaces. The inhomogeneous surface of conducting polymers with local variations in roughness and surface charge can render vesicle fusion over large areas challenging. A good example is the inability to form bacterial native membranes directly on PEDOT:PSS, given they both possess negatively charged surfaces. As such, alternative methods that are agnostic to the surface properties of the substrate have been introduced to overcome the aforementioned issues for SLB formation. One characteristic example is solvent-assisted lipid bilayer formation.[7] However, this method requires the use of solvents that can adversely affect protein functionality and so is not ideal for the study of transmembrane proteins.

Herein, we introduce a simple and versatile method to tune the surface properties of the most commonly used CP in bioelectronics, PEDOT:PSS. While in the context of this work, we primarily applied our approach to PEDOT:PSS based supports, the same surface functionalization method could be extended to all supports that can be hydroxyl-functionalized upon oxygen plasma treatment, including all electroactive polymers[8] and commonly used inorganic substrates such as glass, PDMS (polydimethylsiloxane), or silicon.[9] By tailoring the surface chemistry of the CP, we optimize the electrostatic and van der Waals interactions between the substrate and the lipid bilayer. Since the rupture of lipid vesicles largely depends on such forces, our method shows a clear improvement in SLB coverage and electrical properties of SLBs formed on treated as compared to pristine substrates. This is particularly relevant for PEDOT:PSS-based bioelectronic devices that consist of electrode or transistor arrays which are inherently inhomogeneous in terms of roughness or surface chemistry due to the nature of the PEDOT:PSS blend.[10] A thin (≈ 4 nm, Figure S1, Supporting Information) oligoethylene glycol monolayer is introduced on top of the bioelectronic devices using this approach, providing a homogenous coating that favors lipid–substrate interactions, thus facilitating vesicle fusion while maintaining unchanged electrical properties.[11] With this approach, we avoid the use of polyethylene glycol (PEG, a synthetic polymer not found in cell membranes) either embedded in the lipid vesicles[12] or externally added in solution form[4a,b] in order to promote SLB formation and/or improve coverage as typically shown in previous studies. We showcase the effectiveness of our surface functionalization using biomembranes consisting purely of lipids (1-palmitoyl-2-oleoyl-sn-glycero-3-phosphocholine or POPC) as well as native ones from human embryonic kidney (HEK-293) and murine mouse (17-CL1) cells. Finally, using the 17-CL1-derived cell membranes, we investigate the binding and fusion of mouse hepatitis virus (MHV) to those membranes using our bioelectronic chips. MHV serves as a safe and well-studied coronavirus model that infects mice. We show that the viral entry (i.e., initial receptor
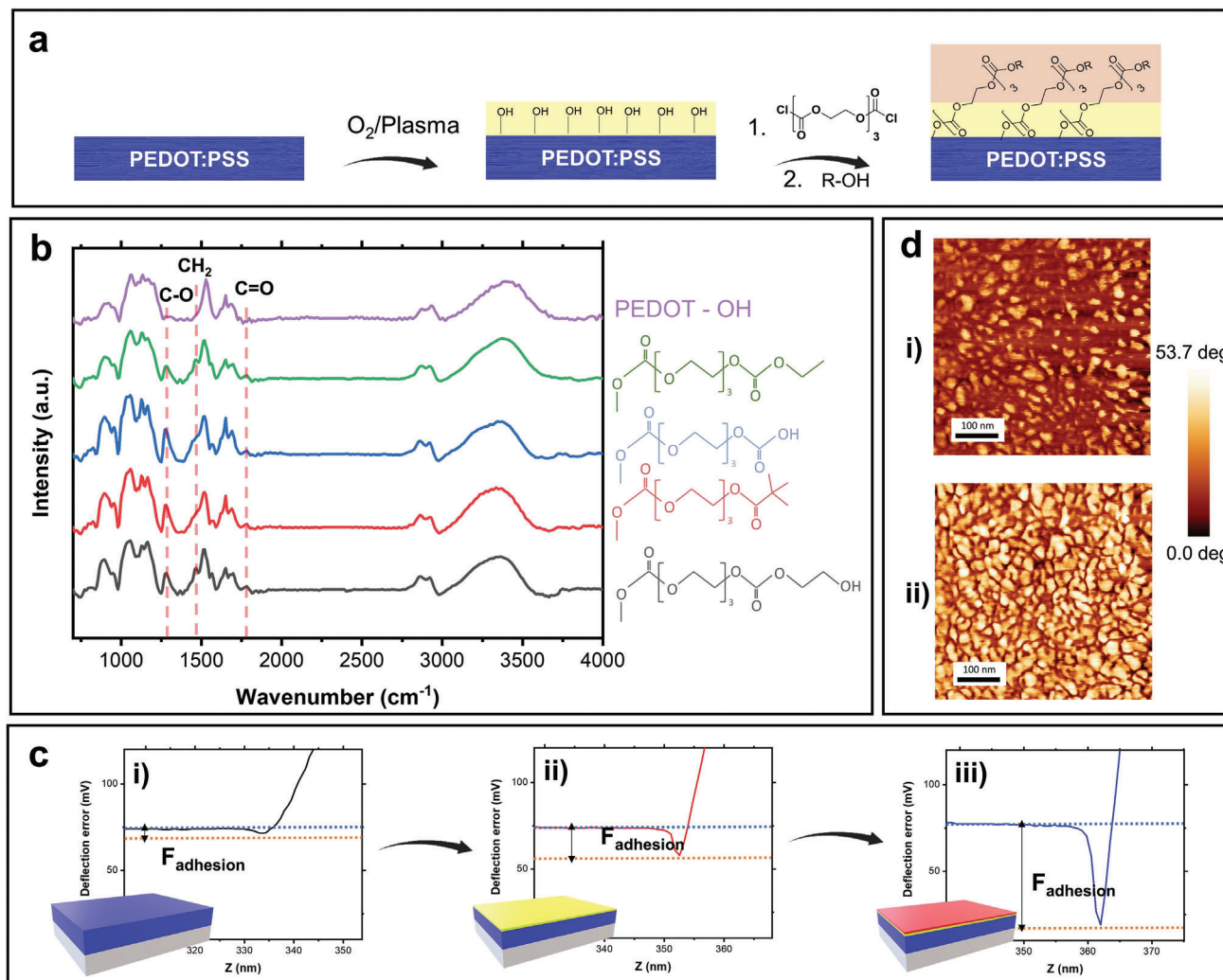
binding and subsequent fusion) can be electrically monitored by recording the membrane resistance. The surface-modified devices exhibit substantially improved signals compared to their non-modified counterparts, possibly due to the higher degree of SLB coverage and thus receptor abundance. The purpose of this technology is to provide a tool to evaluate the efficacy of drugs under development during the earlier stages of the process, when the cost of failure is still low. That is made possible since the vast majority of all approved drugs target proteins on the plasma membrane.[13]

2. Results and Discussion

2.1. Optimizing the Surface Chemistry of PEDOT:PSS to Promote SLB Formation

The general approach that has been followed in order to tailor the surface chemistry of poly(3,4-ethylenedioxythiophene) polystyrenesulfonate (PEDOT:PSS) thin films is shown in **Figure 1**a. First, the polymer films are exposed to mild O_2 plasma treatment introducing hydroxyl groups on their surface,[14] which facilitate in a subsequent step the covalent grafting of a bifunctional (carbonyl chloride) oligoethylene glycol (OEG) monolayer. Finally, the unreacted end of the attached monolayer acts as a capping site, allowing its final functionalization with different alcohol- or amine-containing functional groups, such as alkyl ($–C_xH_y$), hydroxyl ($–OH$), and carboxyl groups ($–COOH$). The success of the grafting reaction is confirmed using Fourier-transform infrared (FTIR) spectroscopy at each step of the process. Figure 1b shows the reflection FTIR spectra obtained for all samples studied during this work. All spectra show similar FTIR bands to PEDOT:PSS. The band at 1515 cm^{-1} can be assigned to the C=C stretching vibration band of the EDOT ring, while the bands centered at 1088 and 3450 cm^{-1} correspond to the C–O–C stretching vibration band of the EDOT ring and the acidic O-H stretching band, respectively.[15] The presence of the PEDOT:PSS-related bands in all the samples studied confirms the stability of the conducting polymer film during the functionalization process. The introduction of the different chemical functionalities is confirmed by the corresponding FTIR spectra. Thus, the FTIR spectra of all the functionalized samples show the presence of a new strong band, centered around 1250 cm^{-1}, which is assigned to the C–O stretching band and corresponds to the new acyl bonds created by the reaction of the bifunctional oligoethylene oxide with the –OH groups present at the surface of the PEDOT:PSS film. Moreover, the presence of new bands at 1450 and 1720 cm^{-1}, corresponding to the C–H bending vibrations of CH_2 and CH_3 groups and C = O stretching bands, respectively, confirms the successful incorporation of the new functional groups on the polymer film.

The ultimate goal of surface modification is to promote SLB formation. The hydrophilic nature of the triethylene glycol chains introduced facilitates the formation of a thin water layer, essential to the mobility of the bilayer, while the presence of different functional groups determines electrostatic and van der Waals interactions between the surface and the lipid vesicles, tailoring their ability to fuse on solid supports.[16] To study the intermolecular interactions present at the surface of the functionalized PEDOT:PSS films, we perform atomic force microscopy

**ADVANCED
SCIENCE NEWS**

www.advancedsciencenews.com

[M] acro-
molecular
Materials and Engineering
Open Access

www.mame-journal.de

Figure 1. PEDOT:PSS films' surface functionalization and characterization. a) Schematic illustration of the functionalization process. PEDOT:PSS film is exposed to O_2 plasma in order to induce the formation of hydroxyl groups on the film surface. In a subsequent step, the film is functionalized with different functional groups following the procedure described in the experimental part. b) FTIR spectra of all the films presented in this work. c) Force–distance AFM curves obtained for the i) pristine PEDOT:PSS; ii) hydroxyl-functionalized PEDOT:PSS, and iii) OEG functionalized—EG capped PEDOT:PSS surface, respectively. d) AFM phase image of i) hydroxyl- and ii) OEG-functionalized—EG capped PEDOT:PSS surface, respectively.

(AFM) measurements of adhesion forces (Figure S2, Supporting Information). Since the AFM tip is hydroxyl functionalized and thus hydrophilic, this technique can provide a proxy to the interaction between the substrate and hydrophilic moieties such as the heads of the liposomes. The weakest adhesion force is observed, as expected, on the unmodified PEDOT:PSS surface (Figure 1c), while the strongest one corresponds to the film functionalized with carboxylic acid groups. This can be explained by the interaction between the -OH groups present at the surface of the standard Si AFM tip used for this study and the different functional groups introduced during the surface functionalization. The presence of hydrophilic groups, that is, carboxyl or hydroxyl groups in the case of the ethylene glycol (EG) (Figure 1c) promotes a significant increase of the adhesion force. On the contrary, the presence of hydrophobic end groups (-CH₃) decreases the adhesion forces between the AFM tip and the PEDOT:PSS surface (Figure S2, Supporting Information). This result confirms the impact that the end group has, to the affinity of the surface to hydrophilic moieties. The impact of the surface functionalization on the electrical properties of PEDOT:PSS-based devices and therefore their sensing capabilities were assessed by electrochemical impedance spectroscopy (EIS). Devices functionalized with -COOH end-groups (H_2O capping) even exhibit lower impedance at high frequencies (Figure S3, Supporting Information), which would increase the sensitivity in a variety of biosensing applications, while the -COOH end-groups simultaneously act as biorecognition elements for a variety of analytes.[17] In order to check the homogeneity of the surface, functionalized and non-functionalized PEDOT:PSS films were also characterized by conventional AFM. AFM phase micrographs of the OEG-functionalized surfaces show a clear change in phase values when compared with the non-functionalized PEDOT:PSS surfaces (Figure 1d), confirming that the functionalization occurs throughout the polymer film surface.

ADVANCED
SCIENCE NEWS

www.advancedsciencenews.com

{M} acro-
olecular
Materials and Engineering

www.mame-journal.de

Table 1. Effect of end-capping groups with varying affinity to the liposomes on the coverage (assessed by fluorescence microscopy) and on the membrane mobility (assessed by FRAP), monitoring the formation of a 1-palmitoyl-2-oleoyl-sn-glycero-3-phosphocholine SLB.

Capping agent	End group	Coverage	Mobility
H_2O	$-COO^-$	✓	✗
EtOH	$-COO-CH_2CH_3$	✗	✗
IPA	$-COO-C-$ $(CH_3)3$	✗	✗
EG	$-COO-CH_2-$ CH_2-OH	✓	✓

Typically, the lateral mobility of the lipids within the membrane is assessed using optical methods such as fluorescent recovery after photobleaching (FRAP). The transparency of PEDOT:PSS films facilitates such optical assessment methods. For the assessment of the lateral mobility of the bio-membranes, lipids in the blebs and liposomes are labeled with a lipophilic fluorescent molecule (R18). Capping groups with varying affinity to the bilayer are tested and evaluated on two grounds: their SLB forming ability in terms of coverage and the mobility of the resulting bilayer. To favor the formation of the bilayer while maintaining the native lateral mobility, the right balance regarding the strength of the interaction between the lipids and the functional groups has to be achieved as described in **Table 1**. On the one hand, the strong interactions obtained through the carboxyl end-functionalization promote the formation of the bilayers even on rough substrates[16a] (Figure S4, Supporting Information). However, the resulting lipid bilayers lose their lateral mobility and therefore their biomimetic character. On the other hand, aliphatic end-groups prevent bilayer formation due to their hydrophobic character. Weak but favorable interactions as obtained by the ethylene glycol end-capping appear to facilitate bilayer formation, while retaining the lateral mobility as indicated by the FRAP measurements (Figure S5, Supporting Information).

Since the ultimate goal of those devices is the label-free transduction of membrane biological events, the bilayers were also characterized using EIS. The EIS data obtained are typically fitted using an equivalent circuit model where PEDOT:PSS is modeled as a capacitor,[18] the electrolyte as a resistor (including the resistance of PEDOT:PSS since those are connected in series), and the biomembrane as a capacitor connected in parallel with a resistor (**Figure 2**a,e).[4a,b] Typically, the resistance of the resulting SLB has been used as a figure of merit, reflecting changes in the ion permeability of the SLB as a result of different types of interactions between the SLB and exogenous compounds (i.e., drugs, toxins, etc.).[4a,b]
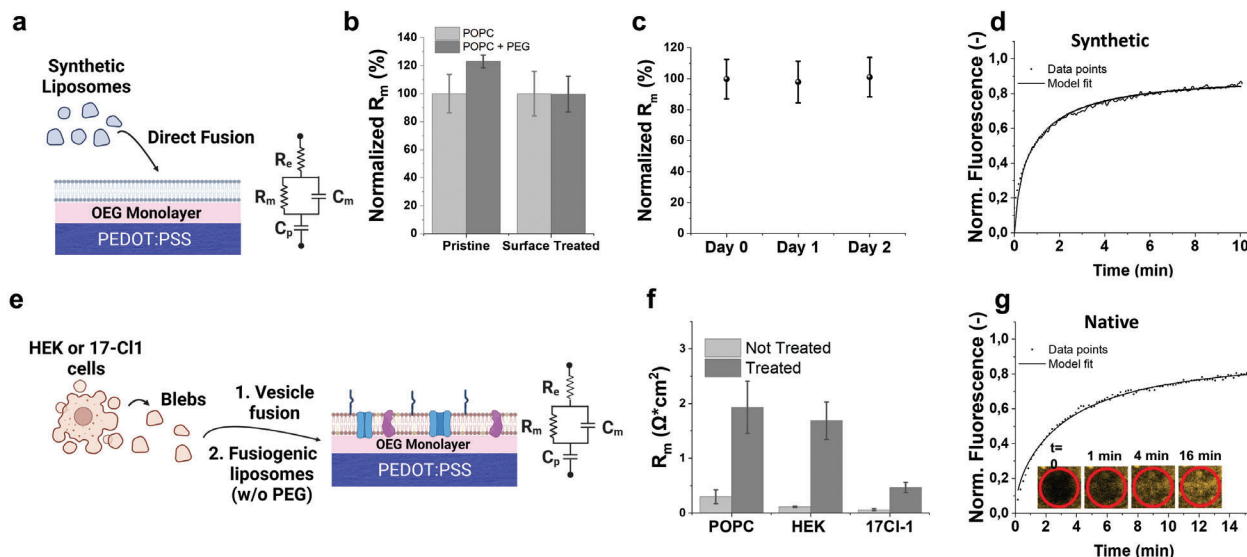
Initially, synthetic SLBs were formed on both pristine and surface-treated PEDOT:PSS-based electrodes (Figure 2a), and the results were again compared using EIS. We note that traditionally, in order to form defect-free SLBs on PEDOT:PSS surfaces, PEG is added, after the addition of the lipid vesicles, acting as a healing agent. This is evident by the typical increase in the calculated resistance of the SLB after PEG addition.[4a] However, in the case of the functionalized PEDOT:PSS surface, PEG is no longer necessary as it does not affect the membrane resistance (Figure 2b). As PEG addition brings additional complexity to our system possibly affecting the EIS data, by avoiding adding it, our approach is significantly simplified. The PEG-free synthetic bilayers formed on the surface-treated devices were found to be stable over a prolonged period of time (when stored at 4 °C) as verified by EIS (Figure 2c), further signifying their stability and robustness without necessitating the addition of a healing/stabilizing agent. Additionally, the lateral mobility of the formed SLBs was verified by FRAP, as shown in Figure 2d. As a next step, native SLBs (formed from human embryonic kidney [HEK] and murine 17Cl-1 derived extracellular vesicles, Figure 2e) were formed on pristine and surface-treated devices and the results were again compared using EIS (Figure 2f). The increased membrane resistance values observed in both membrane types in the case of the surface-treated substrates confirm our initial hypothesis that the surface modification facilitates vesicle–substrate interactions enhancing bilayer formation without the need of using PEG. We note that the compared values are based on PEG-healed (on the non-treated) versus no PEG-added (on the treated substrates). FRAP measurements verify the formation of a mobile native lipid bilayer on the surface-functionalized PEDOT:PSS with $D = 0.1983 \pm 0.0325\ \mu m^2\ s^{-1}$, MF = 0.902 ± 0.007 (Figure 2 g), in line with previously reported values using R18 probes.[2b]

2.2. Real-Time Monitoring of Biological Events: Fusion of Murine Coronavirus on Mammalian Native Membranes

We finally sought to perform a biological functional assay using our membrane-on-a-chip devices. The outburst of the COVID-19 pandemic has clearly pointed out an ever-pressing need in developing versatile platforms to assist and re-direct the drug and vaccine development process. The state-of-the-art methods depend either on whole cell assays or during the later stages of drug development on in-vivo tests on lab animals. Both methods are costly and time-consuming as each testing cycle could last for weeks or even months, while animal testing also raises ethical concerns. As an alternative to whole-cell or in-vivo assays, our groups have recently demonstrated that a cell membrane model on an electronic chip could provide real-time and label-free electronic readouts on the viral entry signature.[19] This method, first demonstrated for the influenza virus, could electronically monitor the binding and subsequent fusion (hemifusion) of the virus on the host cell membrane as electronically expressed by an increase in membrane resistance. One of the main advantages of this method is that it can discriminate between infectious and non-infectious particles and would therefore be ideal to provide real-time feedback on the efficacy of both drugs and vaccines under development.

Here, we apply the same biomembrane–chip coupling to monitor the binding and subsequent fusion of MHV-A59 on biomembranes derived from the 17-Cl1 mouse cell line. A schematic representation of MHV fusion on SLB formed on surface-modified PEDOT:PSS-based electrodes, along with the corresponding equivalent circuit is shown in **Figure 3**a. The MHV serves as a safe SARS-CoV-2 surrogate[20] as it only infects mice. The surface of the PEDOT:PSS-based chips is modified to promote vesicle rupture, as described in Figure 2c. While the unmodified devices showed very little increase in terms of membrane resistance (Figures S7 and S8, Supporting Information),

ADVANCED
SCIENCE NEWS
www.advancedsciencenews.com

[M] acro-
olecular
Materials and Engineering
Open Access
www.mame-journal.de

Figure 2. a) Schematic illustration of synthetic SLB formation on a surface-functionalized PEDOT:PSS substrate. b) Effect of PEG addition on the membrane resistance of SLBs formed on pristine and surface-treated PEDOT:PSS devices. All devices were exposed to the same O_2/plasma conditions. c) Synthetic SLB stability on surface-treated devices, as assessed by EIS. d) FRAP measurement of POPC synthetic SLBs on PEDOT:PSS-coated glass slides functionalized with OEG and capped with EG. d) FRAP measurements of synthetic SLB (POPC) formed on a PEDOT:PSS-coated glass slides functionalized with OEG and capped with EG. Schematic illustration of the blebbing and the subsequent vesicle fusion process on top of the surface-functionalized PEDOT:PSS. e) Comparison of the membrane resistance of synthetic and native bilayers formed on untreated (light grey) and surface-functionalized (EG capping, dark grey) PEDOT:PSS devices. f) FRAP measurements of HEK293 SLBs on PEDOT:PSS-coated glass slides functionalized with OEG and capped with EG.
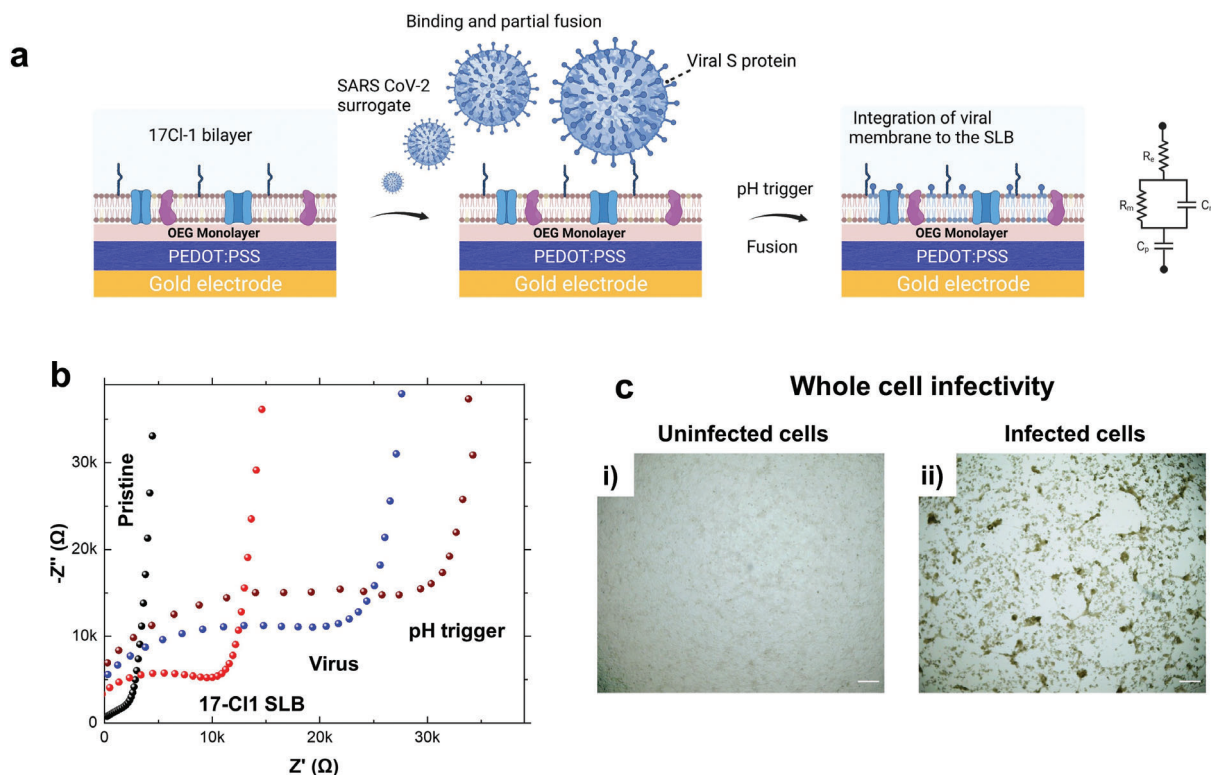
Figure 3. a) Schematic representation of MHV fusion on SLB formed on surface-modified PEDOT:PSS-based electrodes. b) Real-time electrical monitoring of viral fusion on the SLB by EIS (Nyquist). c) Cytopathic effect on 17-Cl1 cells during MHV-A59 infection (100 µm scale bars): i) Uninfected 17-Cl1 cells form a continuous monolayer; ii) infected 17-Cl1 cells show a strong CPE after 48 h.

ADVANCED
SCIENCE NEWS

www.advancedsciencenews.com

{M}acro-molecular
Materials and Engineering
Open Access

www.mame-journal.de

the surface-treated ones yielded a 150% increase in resistance (i.e., from 0.36 to 0.90 Ω cm^2). Figure 3b shows the typical EIS data in the form of Nyquist plot obtained in a treated device after incubation with the MHV virus and after changing the buffer pH to 5.5. We observe a notable increase in the membrane resistance after incubation with the virus (i.e., from 0.36 to 0.65 Ω cm^2) suggesting that virus fusion occurs on the plasma membrane, in line with similar observations with the flu virus.[19] When the pH of the electrolyte is set to 5.5 (simulating the cytosol where the viral S glycoproteins undergo a conformational change that facilitates fusion[21]), we observe an additional increase in the resistance (i.e., from 0.65 to 0.90 Ω cm^2), which could be attributed to virus fusion with the membrane. This is in line with recent studies, where both the endosomal[21] and non-endosomal[22] pathways have been proposed to take place upon virus binding to the cell. It is worth noting that the magnitude of change after viral fusion in the treated versus the untreated devices (see Figure S7, Supporting Information) is considerably higher possibly due to the improved SLB coverage and hence an increased presence of cell membrane receptors for virus binding. To verify the infectivity of the virus, a cytopathic effect assay was carried out on intact 17-Cl1 cells clearly showing the affected cells 48 h after infection (Figure 3c). Finally, in order to assess the specificity of viral binding/fusion to the murine cell-derived membranes, the virus was incubated on membranes made of synthetic liposomes containing no receptors. As shown in Figures S9 and S10, Supporting Information, the membrane resistance after incubation with the virus remains almost unchanged, as expected, as a result of the lack of specific receptors. Taken altogether, our results suggest that this platform has the potential to provide valuable feedback during the early stages of drug development based on the affinity of pathogens with the reconstituted SLBs in the presence of different drugs. Additionally, the surface functionalization of the electronic chip prior to the formation of the biomembrane plays a critical role in increasing receptor abundance and thus amplifying the recorded signals.

3. Conclusions

We report on a general surface functionalization method to facilitate native cell membrane formation on top of electronic chips. Bioelectronic devices and, even more so, organic bioelectronics have been proven invaluable in bridging the communication (ions to electrons) and mechanical (soft to rigid) mismatches between electronics and biological systems using the now standard organic bioelectronic chips.[23] Our approach goes a step further and allows for the tailoring of the surface properties of the electronic chip to match those of the biological substance (i.e., of the SLB). Although we only demonstrated the possibility to modify the surface of PEDOT:PSS, the same approach could be applied to all other electroactive supports conditional on being able to get hydroxyl-functionalized upon exposure to oxygen plasma or a similar method. Another advantage of this method is its versatility in terms of grafted moieties. Here, we demonstrated the grafting of simple molecules on the electronic chips. However, the same approach could be employed for the grafting of more complex molecules with biological activity such as aptamers, enzymes, proteins, and so on, a task that is currently under investigation. On the biological application side, our surface functionalization method facilitates vesicle fusion on top of the electronic chip, greatly improving the capabilities of our devices to monitor biological phenomena, such as the fusion of viruses which can provide a valuable alternative to the state-of-the-art methods for drug and vaccine development.

4. Experimental Section

Preparation of PEDOT:PSS-Coated Glass Slides: The glass slides were sonicated in an acetone/isopropanol (80/20) bath for 10 min and then sonicated in DI water for a further 20 min. They were then dried with a nitrogen gun and treated with oxygen plasma (Harrick Plasma, Ithaca, NY) for 2 min at 18 W. The PEDOT:PSS mixture contained 95% v/v Clevios PH 1000 (Heraeus), 5% v/v ethylene glycol (Sigma-Aldrich), 0.002% v/v 4 dodecylbenzenesulfonic acid (Sigma-Aldrich), and 1% v/v (3-glycidyloxypropyl) trimethoxysilane (Sigma-Aldrich). PEDOT:PSS was spin cast on glass slides (dried under nitrogen and treated with oxygen plasma for 2 min just prior to use) at 2500 rpm for 35 s and baked at 140 °C for 1 h, followed by DI water immersion for 4 h. A glass well was attached with PDMS to retain the buffer solutions.

Device Fabrication: Glass wafers were cleaned in a 90:10 vol/vol sulfuric acid/hydrogen peroxide solution heated at 120 °C for 20 min. A Ti (5 nm)/Au (50 nm)/Ti (5 nm) layer was deposited by e-beam evaporation on top of a photoresist/lift-off resist bilayer pre-patterned by photolithography, followed by lift-off in solvent. The two thin Ti layers act as adhesion layers between Au and the substrate and top insulator. A 100 nm SiO$_2$ insulation layer was deposited by plasma-enhanced chemical vapor deposition and the underlying Au contacts were exposed using photolithography and CHF$_3$ reactive ion etching. A PEDOT:PSS (Clevios PH1000) solution containing 5 vol% ethylene glycol and 1 vol% (3-glycidyloxypropyl)trimethyloxy-silane was spin-coated at 2000 rpm, baked on a hot plate at 120°C for 20 min, and immersed in methanol for 5 min, followed by rinsing in deionized water. The polymer was then protected by a sacrificial layer of Ge (100 nm) deposited using e-beam evaporation. Photolithography followed by reactive ion etching with CF$_4$ and O$_2$ was used to etch through the Ge and PEDOT:PSS layers, respectively. The Ge sacrificial layer was removed by immersing the chips in deionized water overnight.

Surface Functionalization: PEDOT:PSS-coated glass slides or electrodes with glass wells were treated with oxygen plasma (Harrick Plasma, Ithaca, NY) at 18 W for 2 min. Then, 100 μL of tri(ethylene glycol) bis (chloroformate) (Merck) was directly added to each well and incubated for 20 min. The well was then rinsed with dry acetone, and 100 μL of the capping agent (H$_2$O, EtOH, IPA, EG) was added and incubated for 20 min. The films were then rinsed with DI water and kept hydrated until the formation of the bilayer.

Surface Characterization: Surface adhesion forces and AFM images were obtained on a Veeco Dimension Icon atomic force microscope with a Bruker ScanAsyst Air probe (nominal tip radius 2 nm) in contact mode. AFM probe was calibrated before imaging to determine the deflection sensitivity, spring constant, resonance frequency, and quality factor (Q) of the AFM cantilever in air. The standard calibration of the deflection sensitivity was performed against a clean (100) Si wafer (Microchemicals GMBH, Germany). Film thickness measurements were carried out on a Semilab SE2000 variable angle spectroscopic ellipsometer in the spectral range of 300 to 1000 nm. All data analysis was performed using the Semilabs SEA software (v1.6.2), using a Cauchy dispersion law. FTIR measurements of the samples before and after surface functionalization were performed using an AIM-9000 FTIR (Shimadzu). In order to increase the sample reflectance, gold-coated (100 nm) Si substrates were used during this study.

Virus and Cell Lines: Murine hepatitis virus A59 (MHV-A59) and murine fibroblast cell line 17Cl-1 were kindly donated by Professor Ian Goodfellow, University of Cambridge. 17Cl-1 cells were maintained in Dulbecco's modified Eagle's medium low glucose 1 g L^{-1} (DMEM, Life Technologies) supplemented with 5% fetal bovine serum (Merck), 6% tryptose phosphate broth (Merck), 1x non-essential amino acids (Gibco), 1x antibiotic-antimycotic (Thermo Fisher Scientific), and 1x L-Glutamine

(Gibco). MHV-A59 was propagated by inoculating 17Cl-1 cells at a multiplicity of infection of 0.01 TCID50 per cell. MHV-A59 was harvested by centrifugation at 3000 rpm for 10 min and stored in aliquots at −80 °C. Viral titers were determined by Reed and Muench 50% tissue culture infectious dose (TCID50) end point method. Briefly, a 96-well plate was seeded with 100 µL 17Cl-1 cells 1 day prior to the infection assay. Stock virus was prepared in a tenfold dilution series in inoculation medium (DMEM [Life Technologies], 2.5% fetal bovine serum [Merck], 3% tryptose phosphate broth [Merck], 1x non-essential amino acids [Gibco], 1x antibiotic-antimycotic [Thermo Fisher Scientific], and 1x L-glutamine [Gibco]). Dilutions (50 µL) were added to each well and cells were incubated at 37 °C with 5% CO_2. Cytopathic effect was observed after 48 h.

Human embryonic kidney cells were a kind gift from Marc Borsotto, Universite de Nice Sophia Antipolis. HEK cells were maintained in DMEM with the addition of 10% fetal bovine serum (Merck), 50 U mL^{-1} penicillin and 50 µg mL^{-1} streptomycin (Thermo Fisher Scientific, TFS), 1% v/v GlutaMax (TFS), and 50 µg mL^{-1} gentamicin (TFS).

Preparation of Plasma Cell Membrane Vesicles (Blebs): HEK and MHV cells were seeded in culture dishes (10 cm, Corning) and grown for 24−48 h at 37 °C, 5% CO2 incubator. Cells were then washed with GPMV buffer (2 mM $CaCl_2$, 10 mM HEPES, 150 mM NaCl at pH 7.4) and then incubated with 4 mL of GPMV buffer supplemented with 25 mM formaldehyde (FA) and 2 mM dithiothreitol (DTT) (0.075%FA) to induce the formation of blebs, for 1.5 h at 37 °C. The solution containing the blebs was placed on ice for 15 min to separate cell debris from blebs, which were subsequently collected from the supernatant.

Preparation of Liposomes: 25 mg mL^{-1} of 1-palmitoyl-2-oleoyl-sn-glycero-3-phosphocholine (Avanti Polar Lipids) in chloroform was dried under nitrogen. The lipids were further dried under vacuum in room temperature (1 h) to evaporate the remaining chloroform. Then, the film was resuspended in PBS to a concentration of 4 mg mL^{-1}. The solution was then extruded 21 times through a 50 nm membrane (GE Healthcare).

Formation of Synthetic SLBs: 100 µL of synthetic liposomes (POPC 4% in PBS) were added on a surface-treated PEDOT:PSS-coated glass slide/electrode with an attached glass well. The liposomes were incubated for 45 min and then rinsed with PBS (3x).

Formation of Native SLBs: 100 µL of bleb solution was added on a surface-treated PEDOT:PSS coated glass slide/electrode with an attached glass well. The blebs were incubated for 45 min and then rinsed with PBS (3x). Then 100 µL of synthetic liposomes (POPC 4% in PBS) were added and incubated for another 45 min. After incubation, the bilayers were rinsed with PBS (3x).

FRAP Measurements: FRAP experiments were performed on an inverted Zeiss LSM800 confocal microscope (Zeiss Germany) with a 10× objective. To label the membrane, 1 µL of 0.36 mM octadecyl rhodamine B chloride (R18, Molecular Probes) fluorophore was added to 200 µL of bleb or liposome solution in a sonication bath for 15 min. The excess of fluorophore was removed by using a G25 spin column (GE Healthcare). Starting from the labeled blebs, supported lipid bilayers were assembled as described. A 150 mW 561 nm optically pumped semiconductor laser (Coherent, Inc.) was used to photobleach a 20 µm diameter spot in the supported lipid bilayer, and its fluorescence intensity recovery was monitored up to 20 min. The fluorescence intensity change over time was fit using a Bessel function, following the method of Soumpasis.[24] The diffusion coefficient was calculated with the following equation:

$$D = w^2 / 4t_{1/2} \tag{1}$$

where w is the radius of the photobleached spot and $t_{1/2}$ is the time required to achieve half of the maximum recovery intensity.

Electrochemical Impedance Spectroscopy: An Autolab PGSTAT128N potentiostat equipped with a frequency response analyzer was used to record impedance spectra at the frequency range between 100 kHz and 1 Hz. Commercial Ag/AgCl and a platinum mesh were used as reference and counter electrodes, respectively. The micro-fabricated PEDOT:PSS-coated Au electrodes were used as the working electrode. The active electrochemical area of the electrodes was 2500 µm^2. An AC voltage of 0.01 V and a DC voltage of 0 V versus OCP (open circuit potential) were applied. All measurements were taken in ≈200 µL PBS retained on the chip by a glass well.

Electrochemical Monitoring of Viral Fusion: To monitor the viral fusion, EIS measurements were taken on individual electrodes after each step as follows: First bare PEDOT:PSS electrodes were measured. Then, the surface of PEDOT:PSS was functionalized in order to facilitate SLB formation. Subsequently, SLB were formed on the electrodes. After that, the MHV A59 was added and incubated for 5 min on top of the SLB-functionalized devices. The virus was then triggered to fuse by lowering the pH by incubating with a citric acid/MES buffer. Nova software was then used for data analysis and modeling to extract the membrane resistance values.

Supporting Information

Supporting Information is available from the Wiley Online Library or from the author.

Conflict of Interest

The authors declare no conflict of interest.

Author Contributions

K.K. conceptualized the surface functionalization approach. R.M.O., A.S., S.D., and A.-M.P. conceptualized the biological application with the SARS-CoV-2 surrogate. The initial draft was written by K.K., A.-M.P., and A.A.F. A.A.F. performed the surface characterization (IR, AFM, and ellipsometry) supervised by S.G. Q.T. and Z.L. microfabricated the devices used in the context of this study supervised by A.S. and R.M.O., respectively. I.C. maintained the cell cultures and prepared the synthetic liposomes. W.C.T., K.B., and K.K. performed the FRAP experiments and W.C.T. and K.B. analyzed the data. K.K., A.-M.P., and Z.L. performed the EIS measurements, forming the synthetic and native bilayers, and subsequently recording the viral fusion. K.K. analyzed the EIS data. S.S. performed the infectivity assay supervised by G.C. The project was supervised throughout by R.M.O.

Data Availability Statement

The data that support the findings of this study are available from the corresponding author upon reasonable request.

[1] L. K. Tamm, H. M. Mcconnell, *Biophys. J.* **1985**, *47*, 105.

[2] a) C.-Y. Hsia, L. Chen, R. R. Singh, M. P. Delisa, S. Daniel, *Sci. Rep.* **2016**, *6*, 32715; b) M. J. Richards, C.-Y. Hsia, R. R. Singh, H. Haider, J. Kumpf, T. Kawate, S. Daniel, *Langmuir* **2016**, *32*, 2963; c) H.-Y. Liu, H. Grant, H.-L. Hsu, R. Sorkin, F. Bošković, G. Wuite, S. Daniel, *ACS Appl. Mater. Interfaces* **2017**, *9*, 35526.

[3] K. A. Jansen, P. Atherton, C. Ballestrem, *Semin. Cell Dev. Biol.* **2017**, *71*, 75.

[4] a) H.-Y. Liu, A.-M. Pappa, A. Pavia, C. Pitsalidis, Q. Thiburce, A. Salleo, R. M. Owens, S. Daniel, *Langmuir* **2020**, *36*, 7325; b) A.-M. Pappa, H.-Y. Liu, W. Traberg-Christensen, Q. Thiburce, A. Savva, A. Pavia, A. Salleo, S. Daniel, R. M. Owens, *ACS Nano* **2020**, *14*, 12538; c) C. Pitsalidis, A.-M. Pappa, M. Porel, C. M. Artim, G. C. Faria, D. D. Duong, C. A. Alabi, S. Daniel, A. Salleo, R. M. Owens, *Adv. Mater.* **2018**, *30*, 1803130; d) M. Kawan, T. C. Hidalgo, W. Du, A.-M. Pappa, R. M. Owens, I. McCulloch, S. Inal, *Materials Horizons* **2020**, *7*, 2348; e) Z. Lu, D. Van Niekerk, A. Savva, K. Kallitsis, Q. Thiburce, A. Salleo, A.-M. Pappa, R. M. Owens, *J. Mater. Chem. C* **2022**, *10*, 8050.

[5] Y.i Zhang, S. Inal, C.-Y. Hsia, M. Ferro, M. Ferro, S. Daniel, R. M. Owens, *Adv. Funct. Mater.* **2016**, *26*, 7304.

[6] G. J. Hardy, R. Nayak, S. Zauscher, *Curr. Opin. Colloid Interface Sci.* **2013**, *18*, 448.

[7] A. R. Ferhan, B.o K. Yoon, S. Park, T. N. Sut, H. Chin, J. H. Park, J. A. Jackman, N.-J. Cho, *Nat. Protoc.* **2019**, *14*, 2091.

[8] C.-M. Chan, T.-M. Ko, H. Hiraoka, *Surf. Sci. Rep.* **1996**, *24*, 1.

[9] S. Bhattacharya, A. Datta, J. M. Berg, S. Gangopadhyay, *J. Microelectromech. Syst.* **2005**, *14*, 590.

[10] J. Ouyang, C.-W. Chu, F.-C. Chen, Q. Xu, Y. Yang, *Adv. Funct. Mater.* **2005**, *15*, 203.

[11] D. Alemu Mengistie, P.-C. Wang, C.-W. Chu, *J. Mater. Chem. A* **2013**, *1*, 9907.

[12] C.-Y. Hsia, L. Chen, R. R. Singh, M. P. Delisa, S. Daniel, *Sci. Rep.* **2016**, *6*, 32715.

[13] J. P. Overington, B. Al-Lazikani, A. L. Hopkins, *Nat. Rev. Drug Discovery* **2006**, *5*, 993.

[14] D. Ohayon, C. Pitsalidis, A.-M. Pappa, A. Hama, Y.i Zhang, L. Gallais, R. M. Owens, *Adv. Mater. Interfaces* **2017**, *4*, 1700191.

[15] a) S. Xiong, L. Zhang, X. Lu, *Polym. Bull.* **2013**, *70*, 237; b) G. Liu, X. Chen, J. Liu, C. Liu, J. Xu, Q. Jiang, Y. Jia, F. Jiang, X. Duan, P. Liu, *Electrochim. Acta* **2021**, *365*, 137363.

[16] a) P. S. Cremer, S. G. Boxer, *J. Phys. Chem. B* **1999**, *103*, 2554; b) N.-J. Cho, C. W. Frank, B. Kasemo, F. Höök, *Nat. Protoc.* **2010**, *5*, 1096.

[17] J. Lei, H. Ju, *Wiley Interdiscip. Rev.: Nanomed. Nanobiotechnol.* **2010**, *2*, 496.

[18] C. M. Proctor, J. Rivnay, G. G. Malliaras, *J. Polym. Sci., Part B: Polym. Phys.* **2016**, *54*, 1433.

[19] T. Tang, A. Savva, W. C. Traberg, C. Xu, Q. Thiburce, H.-Y. Liu, A.-M. Pappa, E. Martinelli, A. Withers, M. Cornelius, A. Salleo, R. M. Owens, S. Daniel, *ACS Nano* **2021**, *15*, 18142.

[20] R. Körner, M. Majjouti, M. Alcazar, E. Mahabir, *Viruses* **2020**, *12*, 880.

[21] P. Eifart, K. Ludwig, C. Böttcher, C. A. M. De Haan, P. J. M. Rottier, T. Korte, A. Herrmann, *J. Virol.* **2007**, *81*, 10758.

[22] S. T. Hingley, I. Leparc-Goffart, S.u-H. Seo, J. C. Tsai, S. R. Weiss, *J. Neurovirol.* **2002**, *8*, 400.

[23] T. Someya, Z. Bao, G. G. Malliaras, *Nature* **2016**, *540*, 379.

[24] D. M. Soumpasis, *Biophys. J.* **1983**, *41*, 95.